
Research on Wind Energy Fluctuation Stabilization and Hybrid Energy Storage Capacity Optimization Strategy Based on EWD

Zhaorui Lv^{1,*}, Zhiyong Wang², Changhe An¹

¹Mechanical and Electrical Engineering Division, Wenhua College, Wuhan, China

²The Fourth Military Representative Office, NEO, Shanghai, China

Email address:

Navylvzhaorui@163.com (Zhaorui Lv), free_wzy@qq.com (Zhi yong Wang), 13995508451@163.com (Chang he An)

*Corresponding author

To cite this article:

Zhaorui Lv, Zhiyong Wang, Changhe An. (2023). Research on Wind Energy Fluctuation Stabilization and Hybrid Energy Storage Capacity Optimization Strategy Based on EWD. *International Journal of Energy and Power Engineering*, 12(6), 100-108.

<https://doi.org/10.11648/j.ijepe.20231206.13>

Received: November 28, 2023; **Accepted:** December 13, 2023; **Published:** December 22, 2023

Abstract: With the increase of installed capacity of wind power in China, the randomness and fluctuation of wind power output power make the grid frequency modulation more difficult. To solve this problem, a hybrid energy storage system composed of lithium batteries and super-capacitors is used to stabilize the wind power output. This study focuses on the smoothing strategies and capacity configuration methods of hybrid energy storage system, which is of great significance to increase its utilization rate and reduce energy storage capacity. An empirical wavelet decomposition method is used to decompose the wind farm output power data and obtain the charging and discharging instructions of hybrid energy storage system. For the smoothing power of energy storage system, high frequency decomposition is carried out with the lowest cost as the target to obtain the capacity optimization strategy of different types of energy storage. This study also analyzes the typical 8-day output power data of a wind farm and optimizes the power and capacity allocation of lithium battery and supercapacitor through combining numerical examples with wind power system grid power calculation. The numerical examples verify the effectiveness of the proposed smoothing method and capacity optimization algorithm.

Keywords: Wind Power Fluctuation, Hybrid Energy Storage System (HESS), Empirical Wavelet Decomposition (EWD), Empirical Mode Decomposition (EMD), Wavelet Decomposition

1. Introduction

Due to the intermittent and random characteristics of wind energy, the output power of wind power directly incorporated into the power grid will bring negative effects on the stability of the power system, power grid frequency, power quality, power generation planning and dispatching. As a key technical support for a high proportion of new energy connected to the power grid, energy storage is used to smooth the fluctuating power, which can effectively improve the permeability of wind power and grid connection credibility [1-3].

There is great practical significance to use energy storage system to suppress the output power fluctuation of wind farm. Hybrid energy storage system (HESS) uses the combination of energy storage such as battery and power energy storage such

as super-capacitor to suppress the output power fluctuation of wind power generation, so as to increase the utilization rate of the energy storage system and reduce the required capacity of the energy storage system. There are two aspects of research on this type of problem, one is to obtain the target grid power that meets the grid-connection conditions, the other is how to determine the capacity ratio of each energy storage system [4-7].

The primary goal of energy storage to suppress wind power fluctuation power is to obtain the target power by using the control algorithm under the condition of grid connection constraint. In the field of micro-grid where wind energy and energy storage coexist, its power reflects typical non-stationary characteristics, while in the field of local spectrum analysis of non-stationary signals, in order to obtain

the frequency domain characteristics of non-stationary signals, short-time Fourier decomposition and wavelet decomposition are the two main means. Pang Ming et al. [8] used the discrete Fourier transform to analyze the fluctuation characteristics of wind power from the frequency domain perspective. There are also many research results on wind power fluctuation stabilization and hybrid energy storage capacity configuration methods [9-11]. However, due to the window length of the Fourier method and the choice of the wavelet base, it is necessary to adopt the mode decomposition method for unmaned parameters. Therefore, the empirical mode decomposition (EMD) came into being, adapting to both nonlinear and non-stationary signals. The EMD method automatically decomposes the signal into a finite number of empirical modal functions (IMF) based on signal features

component product. Huang N E use Empirical Mode Decomposition and Hilbert Spectral Analysis Method for Nonlinear and Non-stationary Time [12], Sun Cheng chen and others [13] optimized the configuration of the hybrid energy storage capacity of the micro-grid based on EMD and neural network. However, the EMD method is not supported by perfect mathematical theory, and there will be such problems as envelope, under envelope and mode overlapping in the application process.

The empirical wavelet decomposition (EWD) integrates the adaptive decomposition concept of the EMD method and the tight support framework of the wavelet transform theory, providing a new adaptive time-frequency analysis idea for signal processing. At present, EWD method is mainly used in in fault diagnosis and fault information extraction [14, 15].

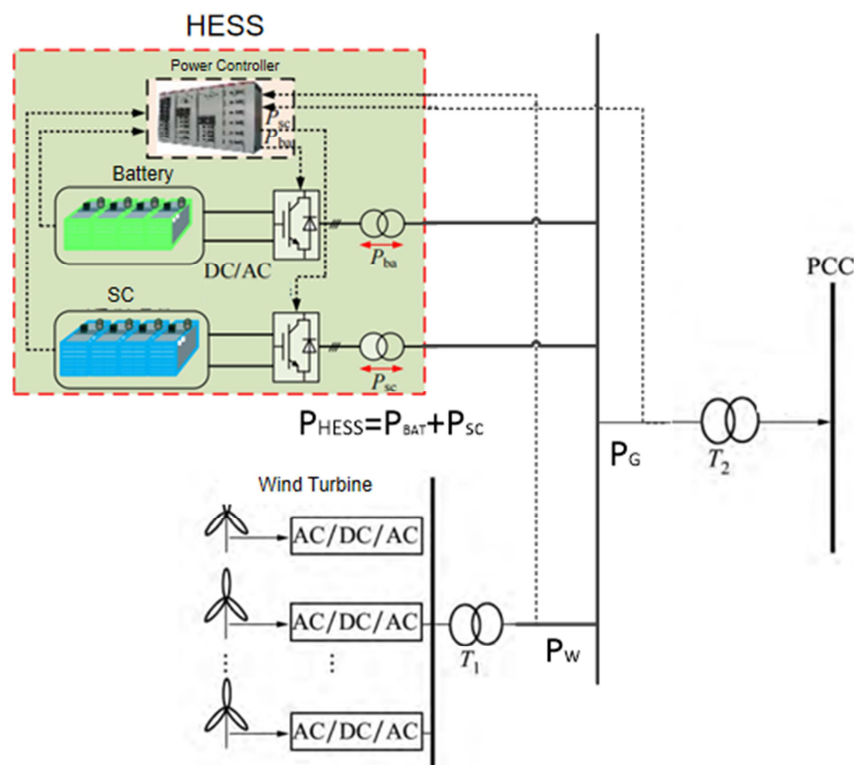


Figure 1. Topology diagram of wind power HESS.

In this paper, a hybrid energy storage system composed of lithium battery and super-capacitors is used to suppress the active power output of the wind farm. The system topology as shown in figure 1, with the wind farm access power system technical regulations as the constraints, the wind farm output experience wavelet decomposition, using low frequency signal decomposition to get grid power and hybrid energy storage power reference. Then the high frequency signal decomposition is used to obtain the power reference value of super-capacitors and lithium battery respectively with the optimal average annual cost of lithium battery and super-capacitors at different decomposition scales. Finally, the typical 8-day power data of a wind farm is used to verify the grid-connected power stabilization effect and the capacity configuration method of hybrid energy storage system.

2. Strategy Introduction

2.1. Wind Energy Fluctuation

The current standard for wind power fluctuation is the limit of active power change of wind farms according to the Technical Regulations on Wind Farm Access to Power System (GB/T19963.1-2021): the maximum change of wind power grid connected power within 1min and 10min shall not exceed 1/10 and 1/3 of the installed capacity of wind farm respectively under the normal operation condition. As shown in Table 1, this is the control target for the grid-connected power fluctuation, and based on this restriction, a reasonable control strategy is designed to reduce the capacity configuration of the hybrid energy storage system.

Table 1. Recommended value of the maximum power change.

Installed capacity of wind farms/MW	Maximum change of 1min /MW	Maximum change of 10min /MW
<30	3	10
30~150	Installed capacity/10	Installed capacity/3
>150	15	50

2.2. Mixed Energy Storage Energy Distribution

Economy is the biggest sore spot of energy storage project

$$\min C_Z = \min\{C_{BAT} + C_{SC}\} \tag{1}$$

Where,

$$C_{BAT} = C_{BATT} + C_{BATY} = (k_{BP}P_{BAT} + k_{Be}E_{BAT}) \frac{r_0(1+r_0)^{N_{BY}}}{(1+r_0)^{N_{BY}-1}} + k_{By}E_{BAT}$$

$$C_{SC} = C_{SCT} + C_{SCY} = (k_{BCp}P_{SC} + k_{Ce}E_{SC}) \frac{r_0(1+r_0)^{N_{CY}}}{(1+r_0)^{N_{CY}-1}} + k_{Cy}E_{SC}$$

In the formula: C_Z is annual comprehensive cost of the system, C_{BAT}, C_{SC} are Lithium battery investment cost and maintenance cost, super-capacitor investment cost and maintenance cost respectively, $C_{BATT}, C_{BATY}, C_{SCT}, C_{SCY}$ represents the initial investment cost and annual maintenance cost of lithium batteries and super-capacitors; $P_{BAT}, E_{BAT}, P_{SC}, E_{SC}$ represents the rated power and rated capacity of lithium battery and super-capacitor respectively, $k_{BP}, k_{Be}, k_{By}, k_{CP}, k_{Ce}, k_{CY}$ represents the power cost coefficient, capacity cost coefficient, maintenance cost coefficient of lithium battery and super-capacitor, r_0 is the discount rate.

3. Empirical Wavelet Decomposition

The EWD is a non-stationary signal processing method proposed by Gilles in 2013. Compared with EMD method, EWD method can overcome the mode overlapping problem caused by the discontinuity of signal time and frequency scale. Meanwhile, it has a complete and reliable mathematical theory basis and low computational complexity.

To achieve the adaptation of signal analysis, EWT uses the information on the frequency spectrum of the analyzed signal to calculate the desired form of the desired band-pass filter. First, we gauge the frequency range to $[0, \pi]$, assuming that

application, and hybrid energy storage system capacity optimization configuration goal is to target the power required by the energy storage system, rationally allocate the capacity of lithium batteries and supercapacitors, so as to minimize the annual comprehensive cost of the system. This paper is mainly for the grid yard, without temporarily considering electricity cost. The target function can be expressed as formula 1.

the signal is decomposed into N frequency bands, and an N-1 boundary is required in addition to the boundary corresponding to $\omega = 0$ and $\omega = \pi$. In the traditional band division method, the amplitude of the signal spectrum is ranked from large to small, and the first N points and their corresponding frequencies are taken: $\varepsilon_n (n = 1, 2, \dots, N)$. Figure 2 gives the schematic diagram of the band division. The frequency band demarcation frequency calculation formula is as equation 2.

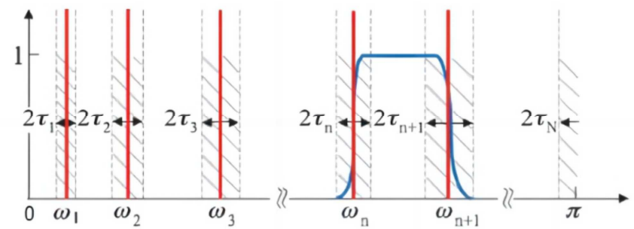


Figure 2. Schematic diagram of the frequency band division.

$$\omega_n = \frac{\varepsilon_n + \varepsilon_{n+1}}{2} \tag{2}$$

For any $n > 0$, the empirical wavelet generating function and the empirical wavelet sub-function are defined by equations (3) and (4) respectively.

$$\widehat{\psi}_n(\omega) = \begin{cases} 1 & \omega_n + \tau_n \leq |\omega| \leq \omega_{n+1} - \tau_{n+1} \\ \cos\left[\frac{\pi}{2}\beta\left(\frac{1}{2\tau_{n+1}}(|\omega| - \omega_n + \tau_n)\right)\right] & \omega_n - \tau_n \leq |\omega| \leq \omega_{n+1} + \tau_{n+1} \\ \sin\left[\frac{\pi}{2}\beta\left(\frac{1}{2\tau_n}(|\omega| - \omega_n + \tau_n)\right)\right] & \omega_n - \tau_n \leq |\omega| \leq \omega_{n+1} + \tau_{n+1} \\ 0 & \text{otherwise} \end{cases} \tag{3}$$

$$\widehat{\phi}_n(\omega) = \begin{cases} 1 & |\omega| \leq \omega_n - \tau_n \\ \cos\left[\frac{\pi}{2}\beta\left(\frac{1}{2\tau_{n+1}}(|\omega| - \omega_n + \tau_{n+1})\right)\right] & \omega_n - \tau_n \leq |\omega| \leq \omega_n + \tau_n \\ 0 & \text{otherwise} \end{cases} \tag{4}$$

The function $\beta(x)$ is an arbitrary $C^k([0,1])$ function with the following conditions.

$$\beta(x) = \begin{cases} 0, & x \leq 0 \\ 1, & x \geq 1 \end{cases} \tag{5}$$

And, $\beta(x) + \beta(1 - x) = 1 \quad x \in [0, 1]$ (6)

The empirical wavelet transform has a similar definition mode to the classical wavelet transform. Its detail coefficient $W_f^n(n, t)$ and approximate coefficient $W_f^n(0, t)$ are given by the internal product transformation 7 and 8.

$$W_f^\varepsilon(n, t) = \langle f, \psi_n \rangle = \int f(\tau) \overline{\psi_n(\tau - t)} dt \quad (7)$$

$$W_f^\varepsilon(0, t) = \langle f, \phi_1 \rangle = \int f(\tau) \overline{\phi_1(\tau - t)} dt \quad (8)$$

$\bar{()}$ represents the complex conjugate, \langle , \rangle means the inner product.

Thus, the decomposed modal component is made, given by equations 9 and 10.

$$f_0(t) = W_f^\varepsilon(0, t) * \phi_1(t) \quad (9)$$

$$f_k(t) = W_f^\varepsilon(k, t) * \phi_k(t) \quad (10)$$

The signal was reconstructed to obtain equation 11.

$$\tilde{x}(t) = W_f^\varepsilon(0, t) * \phi_1(t) + \sum_{n=1}^N W_f^\varepsilon(k, t) * \phi_k(t) \quad (11)$$

4. Strategy Based on the Empirical Wavelet Decomposition

Combined with the fluctuation limit of wind power grid connection, it is reconstructed into low frequency component and high frequency component.

Low frequency component is defined as equation 12.

$$\left\{ \begin{aligned} IMF_{low1} &= res \\ IMF_{low2} &= IMF_n + res \\ &\vdots \\ IMF_{lown} &= res + IMF_n + \dots + IMF_2 + IMF_1 \end{aligned} \right. \quad (12)$$

The high-frequency component is defined as in Equation 13.

$$\left\{ \begin{aligned} IMF_{high1} &= IMF_1 \\ IMF_{high2} &= IMF_2 + IMF_1 \\ &\vdots \\ IMF_{highn} &= res + IMF_n + \dots + IMF_2 + IMF_1 \end{aligned} \right. \quad (13)$$

The low-frequency component that meets the requirements is directly connected to the grid, the remaining component serves as HESS, as shown in Equation 14.

$$P_W = P_{HESS} + P_G \quad (14)$$

The flow chart of the power task is shown in Figure 3.

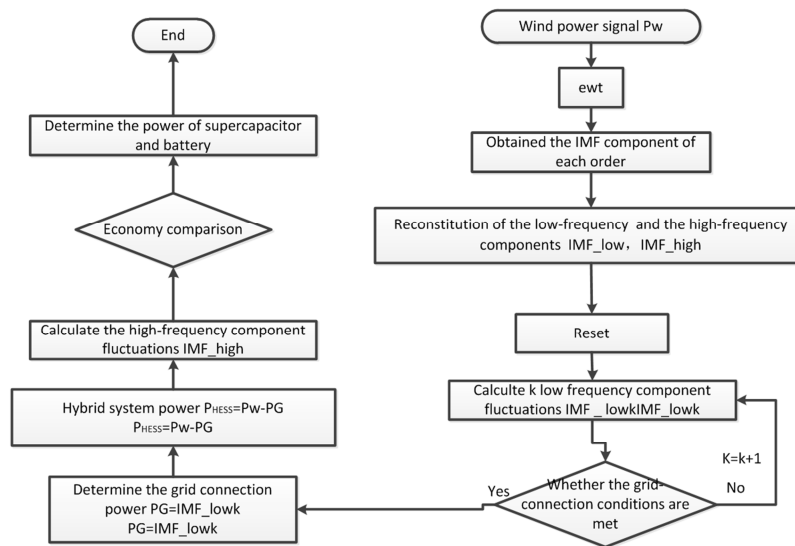


Figure 3. Flow chart of wind energy fluctuation stabilization and optimization strategy.

The specific description is as follows.

- 1) The empirical wavelet decomposition obtained IMF1~IMFn.
 - 2) Reconstitution 1min and 10min low frequency components IMF_low1~IMF_lown.
 - 3) Obtain the maximum value of each low frequency component in 1min, and compared with the power grid suppression limit, the maximum order k1 which is not greater than the limit value is gained.
 - 4) Obtain the maximum value of each low frequency component in 10min, and compared with the power grid suppression limit, the maximum order k10 which is not greater than the limit value is obtained.
- $k = \min(k_1, k_{10})$, the grid-connected power is $P_G =$

IMF_lowk , the HESS requires a stabilization power of P_{HESS} , $P_{HESS} = P_W - P_G = P_W - IMF_lowk = IMF_high(n - k)$.

- 5) After achieving the stabilization power of P_{HESS} , the high-frequency IMF_high 1~ $IMF_high(n - k)$ were investigated separately. Then calculate the annual comprehensive cost, and determine the high decomposition times k' with the lowest cost as the goal, $P_{SC} = IMF_highk'$, thus, $P_{BAT} = P_{HESS} - IMF_highk'$..

5. Example Analysis

Based on the data of every 1 minute of wind power of one

year in a certain district, the paper stabilizes the wind power fluctuation and configures the capacity of batteries and the super-capacitors. The installed wind power capacity is 100MW, and 2 days are selected per quarter, and a total of 8 days are selected as the analysis object in one year.

5.1. Wind Energy Fluctuation

The limit of wind power grid connection fluctuation (according to the recommended value $limit_1=10$, while $limit_{10}=33.3$) used as the dividing line, direct grid connected component and hybrid energy storage power tasks are

obtained. On the basis of 1min of data, the data of ten 1min were averaged to obtain the 10min of wind power generation data for each day. With the 8th day as an example, do empirical wavelet decomposition for 1min and 10 min data, the order is selected as 8, refactoring of its low frequency content, IMF_low1~IMF_low1. The maximum fluctuation quantity of each component is obtained.

As shown in Figure 4, the fluctuation limits of 1min and 10min are shown with different orders. When analyzed from 1min data, $k_1=6$, and correspondingly from 10min data, $k_{10}=4$, then the grid connection power is $P_G = IMF_low4$.

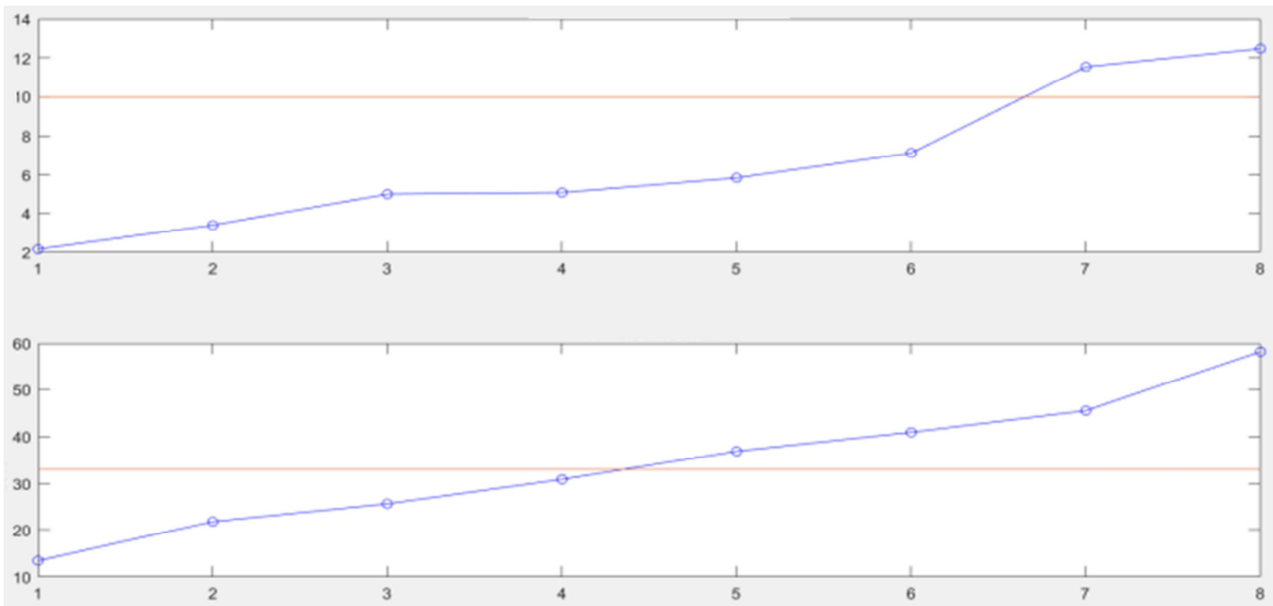


Figure 4. Comparison of the component fluctuations and order in 1min and 10min.

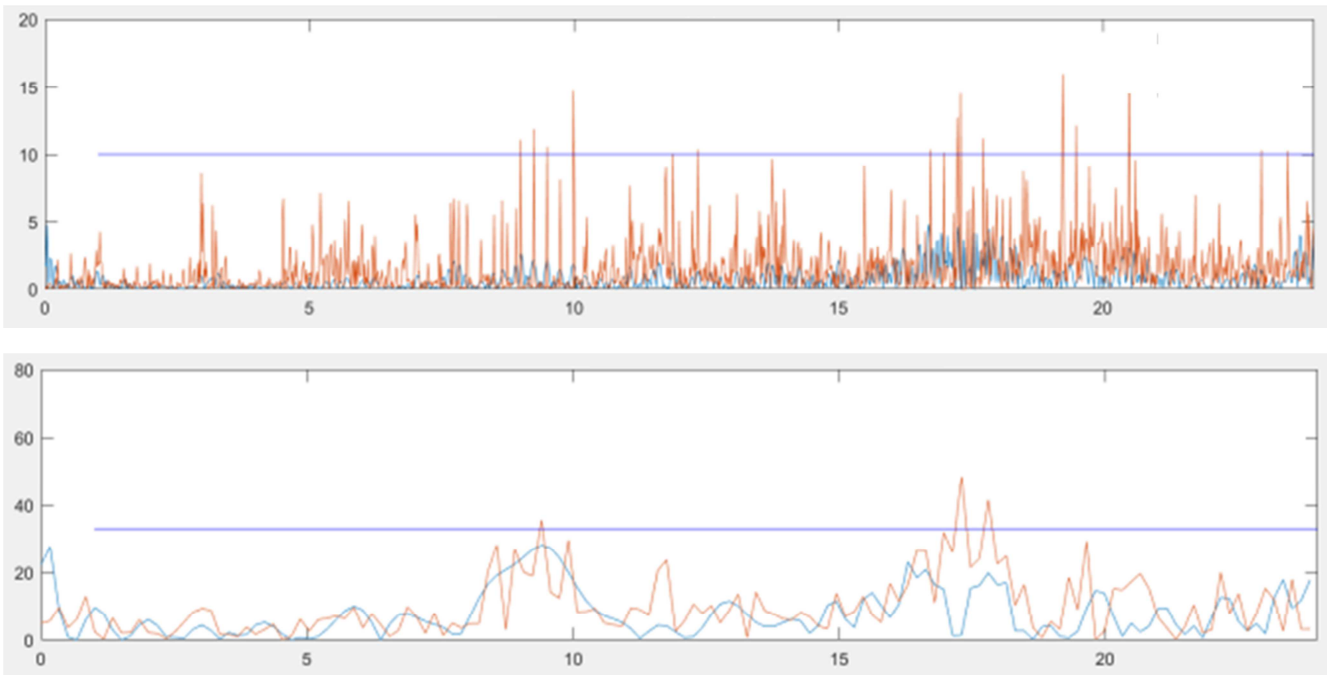


Figure 5. Before and after stabilization (a. 1min, b. 10min) (—Volatility after suppression—Wind power fluctuations—Grid-connected limits).

As shown in Figure 5, a and b are the fluctuations after empirical wavelet decomposition at 1min and 10min

respectively, and the maximum fluctuations of 10min is 30.18MW, which meets the grid connection condition. Meanwhile, the fluctuations of 1min respectively are 5.04MW, which is much less than the grid connection condition of 10MW, reducing the impact of short-time

impact on the energy storage system.

Obtain the grid-connected power and energy storage system stabilization power respectively from the empirical wavelet decomposition of 8 typical daily wind energy power, as shown in Figure 6.

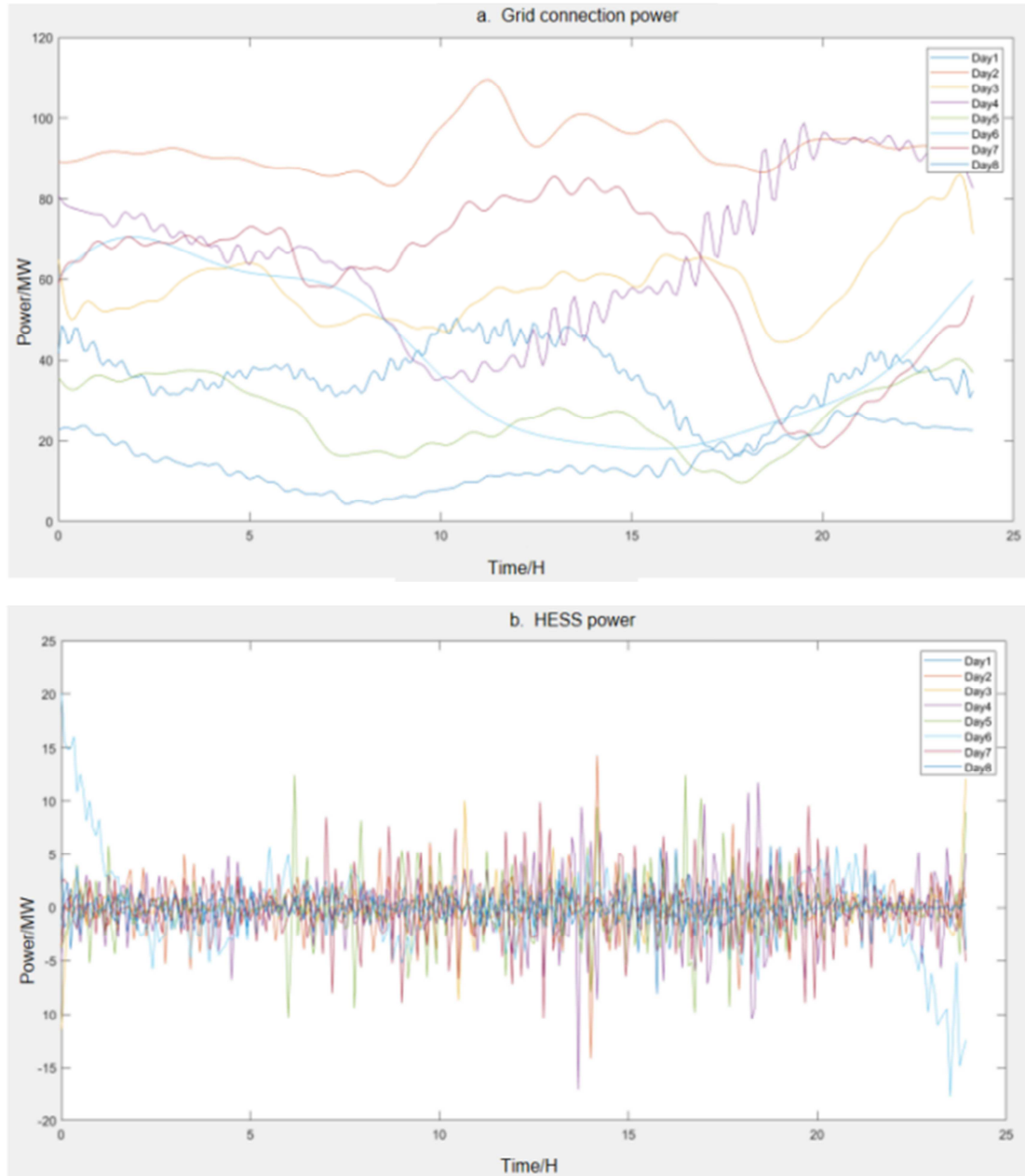


Figure 6. Power (a. Suppression of HESS, b. Grid connection power).

5.2. HESS Energy Distribution

Similarly, take the 8th typical day as the object, investigating the suppression power P_{HESS} , the power cost coefficient of lithium battery is 2.7million CNY/MW, the capacity cost coefficient is 0.64million CNY/MWh, the

power cost coefficient of supercapacitor is 1.5 million CNY/MW, the capacity cost coefficient is 12 million CNY/MWh; the set operating life is $\gamma=15$ years, the discount rate is $r_0=0.06$, and the operation and maintenance cost coefficient is 500 CNY / MWh.

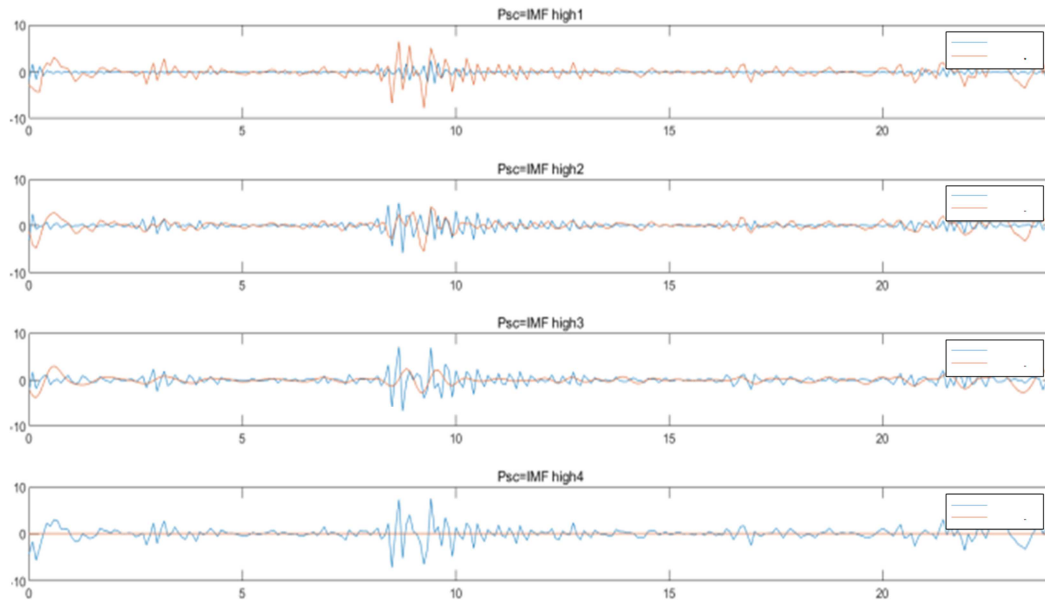


Figure 7. Battery and super-capacitor power under different decomposition modes of the 8th typical day (—SC—BAT).

Table 2. Hybrid energy storage capacity configuration and cost table of the 8th Typical day.

	PSC=IMF_high1		PSC=IMF_high2		PSC=IMF_high3		PSC=IMF_high4	
	BAT	SC	BAT	SC	BAT	SC	BAT	SC
Power/MW	6.49	1.75	4.98	3.27	2.41	6.88	0	7.57
Capacity/MWh	14.28	0.7	6.48	2.52	1.085	8.26	0	15.90
Single investment cost/m.y	0.933	0.386	0.616	1.229	0.252	3.829	0	7.074
Maintenance costs/m.y	0.007	0.00035	0.0032	0.00126	0.00054	0.0041	0	0.0079
Annual comprehensive cost/m.y	1.327		1.849		4.085		7.082	

The configuration results show that by adopting different ways of decomposing powers, varying cost will incur. In the typical day, when $P_{SC} = IMF1$, the average annual comprehensive cost is the smallest. The following conclusions can be obtained.

- 1) Due to the high capacity cost of supercapacitors, the capacity demand of supercapacitors becomes the most important factor in determining the cost.
- 2) When the fluctuating power of wind power is decomposed in more higher dimensions, the better power and capacity ratio of lithium battery and supercapacitors can be found.
- 3) EWD, like EMD, has certain symmetry up and down the envelope curve in high frequency band, which can greatly reduce the capacity demand of lithium batteries and supercapacitors.
- 4) Compared with $P_{SC} = IMF1$ and $P_{SC} = IMF2$, the cost

of the former scheme is lower, but the second scheme of charge and discharge times of lithium battery is less, which reduces the battery loss to a certain extent, thus increasing its life. In the subsequent research, the change of cost caused by different charge and discharge times can be further considered.

- 5) Based on the high-frequency decomposition of EWD for hybrid energy storage system, the power value of hybrid energy storage system is simple and easy to work compared with the complex optimization algorithm. It can be directly used for the power control of real-time converter, and can also be used for different energy storage media.

Since the suppression power has relatively high frequency, it is difficult to identify the graphics when put them together. Figure 8 gives the reference power waveform of the lithium battery and supercapacitors on the 1st and 2nd typical days.

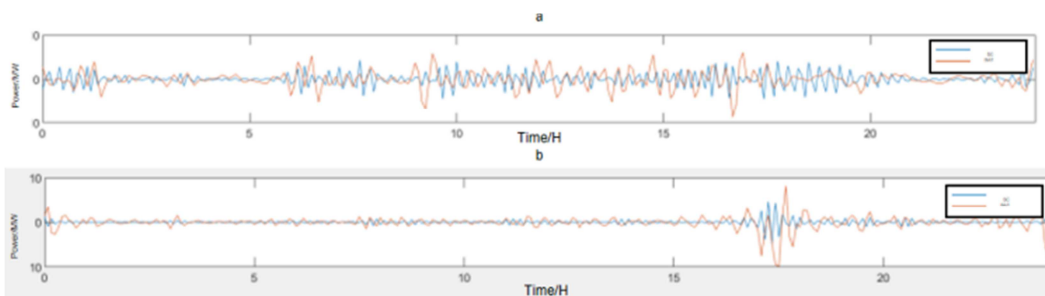


Figure 8. Battery and the supercapacitor power waveform (a. the 1st day, b. the 2nd day) (—SC—BAT).

Table 3. HESS power and capacity configuration table.

	d1	d2	d3	d4	d5	d6	d7	d8
P_BAT/MW	6.21	6.47	5.42	5.66	5.91	10.2	5.78	6.49
E_BAT/MWH	8.69	5.82	4.66	12.45	12.41	8.16	10.80	14.28
P_SC/MW	5.32	5.21	4.73	5.23	2.76	1.4	4.65	1.75
E_SC/MWH	1.59	2.08	1.94	1.67	0.97	0.63	1.39	0.7

Thus, the capacity and power of the wind farm hybrid energy storage system are configured as follows.

$$P_{\text{BAT}} = 6.49\text{MW}, E_{\text{BAT}} = 14.28\text{MWh}$$

$$P_{\text{SC}} = 5.32\text{MW}, E_{\text{SC}} = 2.08\text{MWh}$$

It should be noted that the battery power configuration is 6.49MW, rather than 10.2MW, mainly because 10.2 is far from the data of the other typical days. For economic consideration, 6.49 is selected, and a certain degree of power abandonment will occur in some weather conditions in this configuration. But from the typical data of the year, such discarded electrical energy is economic and realistic.

6. Conclusions

In this paper, the empirical wavelet decomposition is applied to the method of suppressing wind power fluctuation and HESS capacity configuration. The expected output power of the system obtained by the method can meet the active power fluctuation requirements of 1min and 10min of the wind farm, and suppression algorithm can not only be applied to wind farm but also used in photovoltaic power generation. Hybrid energy optimization method can be applied to the configuration of a hybrid energy storage system capacity. Its power command can also be used for real-time power plant power control, which has a very good applicability.

The suppression method and capacity optimization method are consistent and of great practical value. On this basis, the energy storage configuration method considering the uncertain influencing factors such as power abandonment and charge and discharge times can be further studied.

ORCID

Zhaorui Lv: 0009-0003-3059-9237

Funding

Hubei Province First-class undergraduate major construction point Wenhua University of Electrical Engineering and Automation major construction funding project (09 / J09006904).

Conflicts of Interest

The paper claims no conflicts of interest.

References

- [1] Wen Yun feng, Yang Wei feng, Wang Rong hua, et al. Review and prospects of constructing a 100% renewable energy power system [J]. Proceedings of the Chinese Society of Electrical Engineering, 2020, Vol. 40, Iss. 6, pp. 1843-1856.
- [2] Chen Guoping, Li Mingjie, Xu Tao, et al. Study on Technical Bottleneck of New Energy Development [J]. Proceedings of the CSEE, 2017, 37 (1), pp. 20—26.
- [3] Jannati M, Hosseinian S H, Vahidi B, et al. A Survey on Energy Storage Resources Configurations in Order to Propose an Optimum Configuration for Smoothing Fluctuations of Future Large wind Power Plants [J]. Renewable and Sustainable Energy Reviews, 2014, 29, pp. 158-172.
- [4] Li Jianlin, Ma Huimeng, Hui Dong. Present Development Condition and Trends of Energy Storage Technology in the Integration of Distributed Renewable Energy [J]. Transactions of China Electrotechnical Society, 2016, 31 (14), pp. 1-10.
- [5] Tian Jun, Zhu Yongqiang, Chen Caihong. Application of energy storage technologies in distributed generation [J]. Electrical Engineering, 2010, 11 (8), pp. 28-32.
- [6] Qiao Liang bo, Zhang Xiao hu, Sun Xian zhong, et al. Advances in battery-supercapacitor hybrid energy storage system [J]. Energy Storage Science and Technology, 2022, Vol. 11, Iss. 1, pp. 98-106.
- [7] Francisco D G, Andreas S, Oriol G B, et al. A Review of Energy Storage Technologies for Wind Power Applications [J]. Renewable & Sustainable Energy Reviews, 2012, Vol. 16, Iss. 4, pp. 2154-2171.
- [8] Pang Ming, Shi Yikai1, et al. An Optimal Sizing Hybrid Energy Storage System for Smoothing the Output Fluctuations of Wind Power [J]. Journal of Northwestern Polytechnical University, 2016, Vol. 34, Iss. 3, pp. 493-498.
- [9] Wu Xin, Li Yangtao1, et al. Capacity Configuration Method of Hybrid Energy Storage System Based on Improved Wavelet Packet Decomposition [J]. Journal of solar energy, 2023, Vol. 44, Iss. 8, pp. 23-29.
- [10] Li Jie, Yang Lin. Wind power storage capacity configuration based on wavelet transform and chance constrained programming [J]. POWER DSM, 2021, Vol. 23, Iss. 2, pp. 37-42.
- [11] Guo Tingting, Liu You bo, Zhao Jun bo, et al. A dynamic wavelet-based robust wind power smoothing approach using hybrid energy storage system [J]. International Journal of Electrical Power & Energy Systems, 2020, 116, 0142-0615.
- [12] Sun Cheng chen, Yuan Yue, et al. Capacity Optimization of Hybrid Energy Storage System in Microgrid Using Empirical Mode Decomposition and Neural Network [J]. Automation of Electric Power Systems, 2015, Vol. 39, Iss. 8, pp. 19-26.

- [13] Huang N E. New Method for Nonlinear and Nonstationary Time Series Analysis: Empirical Mode Decomposition and Hilbert Spectral Analysis [J]. Proceedings of SPIE-The International Society for Optical Engineering, 2000, pp. 197-209.
- [14] Wang Tao, Zhang Bing. Application of Improved Empirical Transform in Fault Feature Extraction of Bearings [J]. Railway Lowcomtive & Car, 2019, Vol. 39, Iss. 5, 116, pp. 53-58.
- [15] Zhou Hao, Jia Min ping. Analysis of rolling bearing fault diagnosis based on EMD and kurtosis Hilbert envelope demodulation [J]. Journal of Mechanical & Electrical Engineering, 2014, Vol. 31, Iss. 9, 116, pp. 1139-1167.